




Variable Stiffness Actuators for Wearable Applications in Gait Rehabilitation

7

Daniel Gomez-Vargas, Diego Casas-Bocanegra, Marcela Múnera, Flavio Roberti, Ricardo Carelli, and Carlos A. Cifuentes 

7.1 Introduction

Currently, there are mainly two types of robots for rehabilitation and assistance: (1) platform-based robots, intended solely for the improvement of joints function, and (2) wearable devices, which can contribute in the rehabilitation of joints in stationary scenarios, as platform-based robots, but can also improve joints performance during gait in daily activities outside controlled environments. Therefore, this second type of robot exhibits considerable advantages concerning stationary platforms in aspects such as multimodality and applicability [1, 2].

In general terms, devices applied to gait rehabilitation integrate principles implemented in passive orthotic structures, although incorporating the robotics' benefits (i.e., energy supply using actuators, user monitoring through sensors, programmed functionality profiles, among others) [3]. In this sense, those devices mainly aim at improving the patients' gait pattern or decrease the metabolic effort during walking [4]. However, considering the complexity of developing robotic

D. Gomez-Vargas

Biomedical Engineering, Department of the Colombian School of Engineering Julio Garavito, Bogotá D.C., Colombia

Institute of Automatics, National University of San Juan, San Juan, Argentina

e-mail: daniel.gomez-v@mail.escuelaing.edu.co

D. Casas-Bocanegra · M. Múnera · C. A. Cifuentes (✉)

Biomedical Engineering, Department of the Colombian School of Engineering Julio Garavito, Bogotá D.C., Colombia

e-mail: diego.casas-b@mail.escuelaing.edu.co; marcela.munera@escuelaing.edu.co; carlos.cifuentes@escuelaing.edu.co

F. Roberti · R. Carelli

Institute of Automatics, National University of San Juan, San Juan, Argentina

e-mail: froberti@inaut.unsj.edu.ar; rcarelli@inaut.unsj.edu.ar

devices aimed at physical interaction scenarios, wearable devices challenge in aspects such as portability, adaptability to the human body, and compliance [2, 5].

On the other hand, from the capacity of assisting the human body's movements, robotic devices require providing high torque levels during assistive scenarios [6]. Therefore, different actuation systems have been applied in those systems, intending to improve human-robot interaction and assist pathological motor functions. Specifically, current developments integrate principles based on (1) Stiff Actuators, (2) Serial Elastic Actuators (SEAs), and (3) Pneumatic Actuators [4]. Some devices also include other mechanisms such as (4) Hydraulic Actuators and (5) Magnetorheological Actuators [7, 8]. Furthermore, other actuation systems widely implemented nowadays, particularly in wearable systems, applies concepts of (6) Variable Stiffness Actuators (VSAs) and (7) Cable-Driven Actuators [9].

Devices based on pneumatic actuators have potential in aspects such as compliance and physical interaction with the user. However, this actuation type exhibits disadvantages related to the overweight power supply required to assist human movements, as well as hydraulic actuators [9, 10]. On the other hand, wearable robots based on magnetorheological actuators include drawbacks associated with (1) the complex and heavyweight equipment implemented and (2) the high energy consumption to achieve this principle [8].

From the other actuation systems' drawbacks presented above, electrical power supplies could be appropriate for portable devices applied in rehabilitation and assistance scenarios because of their lightweight and autonomy [11]. However, to ensure this portability, those machines need to have reduced sizes and low weights, resulting in a limited torque capacity provided by the system [9]. Consequently, actuators generally include gear mechanisms to enhance the torque capabilities and assist the human body's movements, although reducing the actuator speed response [11]. Nonetheless, the gears' inclusion also leads to non-backdrivable mechanisms, which affect the human-robot interaction [12].

Within the mechanical principles that use electrical power supplies, stiff actuators appear to be an efficient solution to assistive devices. Specifically, this actuation system exhibits relevant characteristics such as high provided torque and wide bandwidth, which are beneficial in assistance applications [13]. Notwithstanding, stiff actuators remain the non-passive backdrivability due to the gears system, resulting in a hard physical interaction [11–13]. Likewise, for human limbs that involve movements in multiple planes, designs with stiff actuators generally restrict several motions, inducing abnormal compensatory movements. Moreover, in terms of interaction, these actuators can present damages derivated from external forces (e.g., impacts or unexpected motions) during real applications [13].

In this context, wearable devices based on cable-driven mechanisms, series elastic actuators, and VSA are emerging to overcome the stiff systems' limitations and preserve the actuators in interaction scenarios. These mechanical principles include elements or mechanisms in the actuator's output to decouple the load, improving the human-robot interaction although reducing the system capacities [9]. This chapter is focused on the VSAs and their potential applications in gait rehabilitation scenarios. The first part explains the variable stiffness principle and

several configurations and techniques to accomplish this behavior. The second part shows the T-FLEX exoskeleton's design based on VSA, and finally, the third part presents two experimental validations in gait assistance and stationary therapy.

7.2 Variable Stiffness Actuators

VSA's concept has arisen from the theory on (1) impedance and (2) Series Elastic Actuators (SEAs) [14], which were published by Hogan [15] and Pratt [13], respectively. Specifically, SEAs involve the spring elements' inclusion between the actuator and the load (see Fig. 7.1a). In this sense, series elastic elements can give back the actuators' lost qualities when it includes a gears system. Geared motors intend to increase the provided torque, reducing the motor speed. However, the gear system introduces characteristics such as (1) high friction, (2) backlash, (3) torque ripple, and (4) noise, affecting the device performance [11, 13].

SEAs work as a low-pass filter for shock loads, reducing peak gear forces [11]. This way, the interaction forces in assistive applications are dissipated mainly by the elastic element, preserving the actuator's mechanical structure. Likewise, this characteristic also affects the torque supplied by the actuator. However, the proper amount of elasticity can solve this drawback without limiting the absorption capability. In terms of control, SEAs turn the force in the impedance concept into a position control problem. Thus, the output force becomes proportional to the position difference across the series elasticity multiplied by its spring constant. Moreover, increased spring constants provide higher control stability, like in a stiff system, even though including the elastic elements' benefits [13].

Actuators based on variable stiffness follow the concept applied in SEAs, where the elastic element is included between the actuator and the load (see Fig. 7.1a). However, the difference lies in the variable impedance's inclusion for the actuator design [14]. This variable impedance allows deviating the equilibrium position (i.e., where the actuator generates zero force or torque) concerning the external forces and the actuators' mechanical properties [16, 17]. This way, VSAs include elastic elements whose spring magnitude takes different values conditioned by an active device (see Fig. 7.1b). Specifically, the adaptive stiffness can be achieved by (1) changing the spring preload, (2) varying the transmission ratio between the output link and the elastic elements, and (3) altering the spring's physical structure [17]. Therefore, this functionality allows adjusting the actuator's stiffness and adapting the device to a specific task [18].

Two setups have mainly been applied in devices that exhibit a variable stiffness behavior: (1) the agonist–antagonist, and (2) the independent motor setup [14]. In the agonist–antagonist principle, two motors modify the stiffness output (see Fig. 7.2b). This way, when actuators turn in the same direction, the output results in movement transmission. On the other hand, when the actuators turn opposite directions, the system exhibits the springs' co-contraction, changing the output stiffness [14, 18]. In terms of design, each motor-spring set is opposite to the other, and usually, the spring size is the same (see Fig. 7.2b).

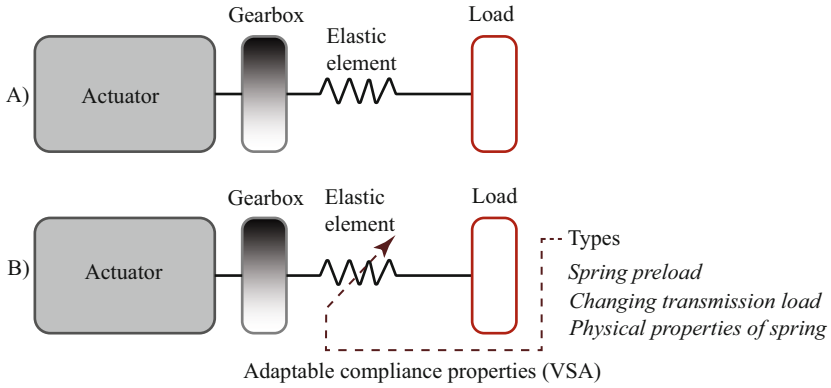


Fig. 7.1 Schematic representation of the actuators studied in this chapter (a) Series Elastic Actuators (SEAs) and (b) Variable Stiffness Actuators (VSAs) in a geared motor

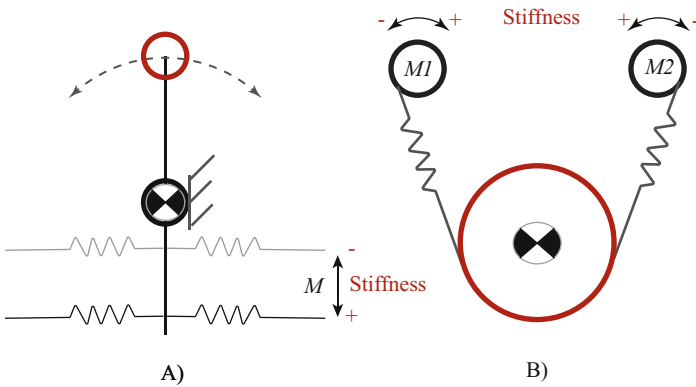


Fig. 7.2 Actuators configurations to generate a variable stiffness behavior. The left part (a) shows the independent motor configuration, and the right part (b) indicates the actuators’ configuration for the agonist–antagonist principle

For a setup with independent motors, a motor varies the output position, resulting in a variable stiffness behavior (see Fig. 7.2a). In this sense, only one actuator is required to change the system’s stiffness concerning the agonist–antagonist configuration. Likewise, that actuator is selected to achieve the needed power for this purpose, which is usually smaller than the primary system’s actuator [14].

The positive effects for the agonist–antagonist configuration effects are related to both motors’ contribution to the stiffness generation [18, 19]. Moreover, for systems that couple tendon-driven mechanisms, this configuration can quickly compensate the stiffness change when the length between the actuator and the joint varies. On the other hand, the independent motor setup ensures smaller and lighter devices because the actuator used to change the stiffness is selected only for this purpose

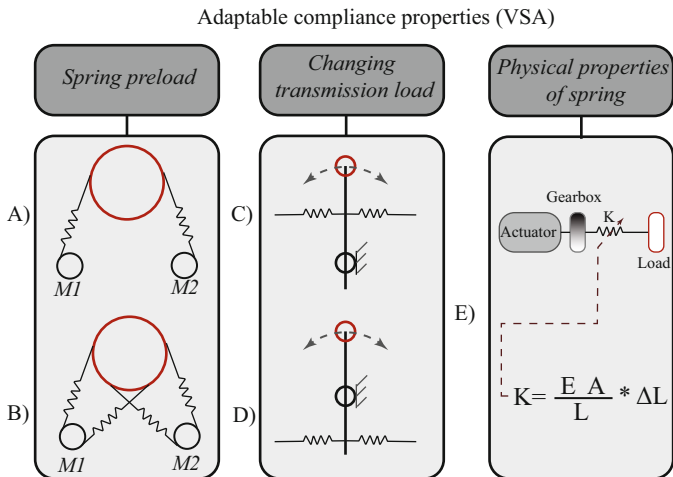


Fig. 7.3 Strategies implemented in a system to change the stiffness. The left part shows the spring preload strategy under agonist–antagonist configuration with two actuators (i.e., M1 and M2). The (c) and (d) parts illustrate the variable stiffness generated by a change in the transmission load. The right part shows the variation in stiffness through the spring’s physical properties (i.e., K parameter shown in Eq. 7.1)

[19]. However, this configuration only uses one motor to move the joint, and consequently, generate the system output torque.

Following these setups, different strategies can be applied to VSAs, looking for changing the system’s stiffness: (1) spring preload, (2) transmission load variation, and (3) spring’s physical properties [14] (see Fig. 7.3).

In the spring preload (see Fig. 7.3a and b), the system response changes concerning the spring pretension. This way, the spring force is directly proportional to the spring displacement, accomplished by the actuator coupled in the system. However, to generate a variable stiffness behavior, energy should be stored in the springs and may not be retrievable. Therefore, an agonist–antagonists setup explained above is implemented, resulting in a large passive angular deflection [14]

For the transmission load variation, the distance between the output link and the spring element (i.e., the transmission ratio) varies continuously, leading to a variable stiffness effect (see Fig. 7.3c and d). Thus, when the springs are close to the pivot, the stiffness is less than when they are far. This strategy does not require energy to change the stiffness because the spring force is orthogonal to the spring displacement [14].

Finally, the variable stiffness strategy is achieved through the spring’s physical properties (see Fig. 7.3e), which is derivated from the basic elasticity law as shown in Eq. 7.1.

$$F = \frac{EA}{L_0} \Delta L = K \Delta L, \tag{7.1}$$

where F is the spring force, E the material modulus, A the cross-sectional area, L the effective beam length, and ΔL is the spring's displacement. Likewise, the stiffness K is defined by EA/L_0 , to control the structural stiffness, any of these parameters should be modified [14]. This way, E is a material property whose change is possible only for some materials through temperature, although this variation is slow. Consequently, the VSA applies changes in the cross-section area and the elastic element's length [14].

Different low-level controllers including position, force, admittance, and impedance controllers have been developed [20]. In this sense, those strategies support elaborate control architectures (i.e., high-level controllers) focused on the actuator's application in real scenarios [9]. In general terms, devices applied to human scenarios require control architectures based on impedance controllers to improve the interaction between the system and the user. In this context, wearable devices based on VSA commonly use position controllers, which inherently results in torque output. This strategy simplifies the force problem to the actuator position problem as in SEAs, being more simple to implement and control [13]. However, considering the non-linearities exhibited by different VSA designs, this strategy could be challenging [16].

7.3 VSA in Rehabilitation Scenarios

Given the possibility of changing the system output stiffness in several interaction cases with the environment (e.g., constant load and constant position) [14], different device's performances can be achieved according to a particular topic. This characteristic is advantageous for VSAs in physical interaction scenarios, something that was a limitation for devices based on SEA [18].

Specifically, in dynamic scenarios, the human body changes its stiffness' properties to accomplish different tasks such as (1) limb movements, (2) shock absorptions, and (3) weight support. Hence, the wearable devices' designs focus on replicating human functions (i.e., bioinspired concepts), intending to improve the physical interaction [21]. Furthermore, spring's inclusion in a system, i.e., based on both SEAs and VSAs, preserves the actuators' mechanisms during scenarios with complex interaction forces (e.g., impacts, mechanical locking, and unexpected events against the actuators' movements) [22, 23]. Likewise, considering the changing stiffness' capability in VSA, the system response could be adapted to modify the user-device interaction during the same task.

In compliance terms, robotic devices applied to rehabilitation scenarios should guarantee safer and more natural interaction with the user [16]. This way, for gait rehabilitation, neurological patients often exhibit sporadic spasms and spastic events. Hence, when robotic devices implement stiff actuators, the response controller tries to correct the position errors generated by those movements. Thus, this correction could cause larger forces, injuring the user's limbs.

Considering the mentioned advantages, this actuation type is widely recommended for robotic applications where the robot interacts intensively with humans

[19,24]. However, despite the benefits of the human–machine interaction, the elastic materials' inclusion limits the actuator's features in terms of bandwidth, supplied torque, response time, among others [25].

Notwithstanding, devices based on VSA allow mitigating the effects caused by the spring's inclusion compared to SEAs. In this sense, higher pretensions lead to a system response similar to a stiff actuator without losing the benefits of spring's inclusion. Hence, system characteristics improve (i.e., increasing the bandwidth and supplied torque and decreasing the response time), and the compliance remains.

In the first part, this section presents different devices that integrate variable stiffness concepts to assist human movements in rehabilitation scenarios. On the other hand, the second part is focused on the T-FLEX ankle exoskeleton, which is a novel bioinspired device based on an agonist–antagonist configuration to achieve a variable stiffness behavior.

7.3.1 VSA in Wearable Robotics

In general terms, robotic devices applied to rehabilitation scenarios arisen from the promising results of including robotics in these applications: (1) neuroplasticity induction, (2) improvement of motor recovery, and (3) regaining functional independence [26–28]. The current developments have been focused on designing soft structures and compliant actuators to guarantee a proper and safer user–device interaction [22]. Specifically, as mentioned previously, wearable devices exhibit benefits regarding platform-based systems regarding a multi-functionality characteristic. Those benefits are mainly related to potential applications of wearable robots in both gait assistance and stationary therapy.

On the other hand, considering the advantages presented in the previous section, wearable devices based on VSA have also shown high potential in rehabilitation scenarios, from the bioinspired operation principle and the system response variation regarding its configuration. In this context, one of the most representative actuators based on VSA concepts is MACCEPA. This actuator consists of 3 bodies pivoting around a common rotation axis whose working principle is a torsion spring able to control its equilibrium position and joint stiffness, independently [23, 29]. Thus, this actuator's design has evidenced high assistance torque levels (i.e., from 50 Nm), comprehensive frequency response (i.e., close to 30 Hz), and consequently, potential use in gait rehabilitation scenarios [23, 30]. Several assistive devices have applied this principle to interact with patients in those scenarios [23, 31–34].

Another actuator focused on gait assistance based on VSA is ARES. This design exhibits relevant characteristics such as lightweight compared to other VSAs, faster response to change the device's stiffness, and considerable assistance torque levels (i.e., providing up to 70 Nm) [30]. ARES includes a stiff set coupled with a compliant mechanism able to change the stiffness using a DC motor. The device aims at controlling the joints' equilibrium position, as occurs in the MACCEPA actuator [35]. ARES has been implemented in the ATLAS exoskeleton, a pediatric device with actuation in the hip, knee, and ankle joints [35, 36].

As well as the previous designs, actuators based on a changing transmission load have also been applied in wearable devices [30, 37]. Specifically, AwAS-II and CompAct-VSA were developed and implemented in lower-limb exoskeletons, including two springs antagonistically attached to the lever that can move toward or away from the pivot [37–39]. In the capacity terms, AwAS-II provides a torque range of 80 Nm with a faster response to adjust the stiffness (i.e., 0.8 s), and CompAct-VSA registers a high torque capacity (i.e., up to 117 Nm) with a faster change stiffness response [30].

In this sense, all of those presented actuators remark the capabilities of devices based on VSA in human interaction scenarios. Notwithstanding, mechanical structures to fix the actuator to the human joints are usually rigid structures that block the joints' movements on the different assisted planes. The following section presents an agonist–antagonist configuration of a VSA ankle exoskeleton with a fully compliant structure.

7.3.2 T-FLEX Ankle Exoskeleton

T-FLEX is a wearable and portable ankle exoskeleton that is part of the AGoRa lower-limb exoskeleton [40]. This device can operate independently (i.e., supporting the ankle movements) or cooperatively with the AGoRA exoskeleton (i.e., assisting the hip, knee, and ankle joints). T-FLEX integrates VSA concepts in its mechanical principle to support the dorsi-plantarflexion movements without restricting the other ankle motions (i.e., foot rotations, inversion–eversion, and pronation–supination) [41]. This exoskeleton integrates two servomotors attached to elastic elements whose mechanical behavior is similar to the human Achilles tendon [42]. It uses an agonist–antagonist configuration with a bidirectional movement mechanism to assist the ankle motions on the sagittal plane (see Fig. 7.4). The principal torque transmission is generated by a composite elastic element that attaches the motor and the user's foot. Moreover, crossed stiff filaments involve both actuators in the torque output, as Fig. 7.4 shows.

The variable stiffness system intends to change the user–device interaction according to the application (i.e., dorsi-plantarflexion repetitions in stationary therapy and gait phases during walking assistance). Likewise, the spring's inclusion also allows modifying the interaction with the patients from their motor capabilities (i.e., increasing initial pretension for a weak ankle or decreasing this value for a spastic ankle). For this purpose, the device includes a composite tendon whose mechanical behavior, tested in stress trials, is similar to the human Achilles tendon (i.e., Young's modulus between 500–1800 Mpa) [42]. The tendon braids flexible materials (i.e., thermoplastic elastomer and fibers of polyethylene) and stiff filaments (i.e., polytetrafluoroethylene) to achieve an exponential stress–strain curve.

The exoskeleton integrates a soft structure, where two actuators are placed on the user's shank (i.e., anterior and posterior sides), as Fig. 7.4 shows. Thus, 3D-printed pieces of polylactic acid (PLA) support the T-FLEX's actuators. Moreover, flexible interfaces of polyurethane-coated, coupled to the support system, improve the

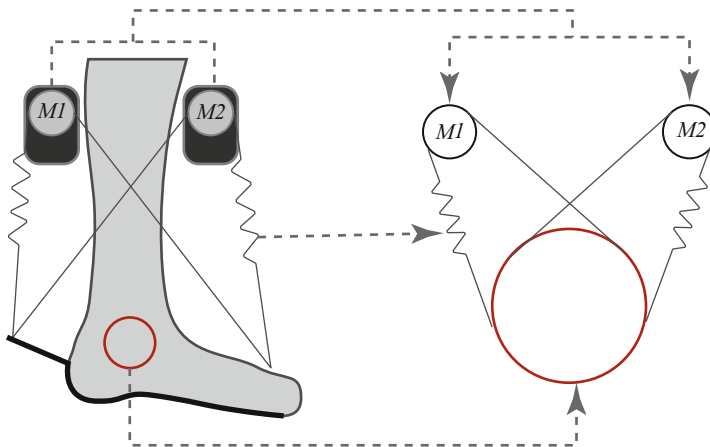


Fig. 7.4 Variable stiffness configuration applied in the T-FLEX exoskeleton. The right part shows the agonist–antagonist setup, including spring elements and stiff filaments. The left part shows this concept implemented on a user’s limb

device-user physical interaction. This way, the device allows portable applications, avoiding slipping and reducing pressure points on the limb related to reaction forces when the device actuates. On the other hand, T-FLEX includes elastic elements and stiff filaments to transmit torque from actuators to the user’s foot. Hence, the exoskeleton uses an insole adapted with 3D-printed pieces to attach the composite tendons to the foot (i.e., heel for plantarflexion and metatarsals for dorsiflexion), as Fig. 7.5. This way, the device comprehends a four-bar mechanism by each actuator, where one of them is a spring with variable stiffness (see Fig. 7.5).

In the electronic system context, the device has two smart servomotors, an inertial sensor, and a processing unit coupled within the open-source robotic meta-operating system (ROS). The actuators are smart servomotors Dynamixel MX106-T (Robotis, Korea) placed on the user’s affected shank (see Fig. 7.6). Each actuator has a stall torque of 10 Nm with a maximum no-load speed of 55 rpm for a power supply of 14.8 V.

The sensing system integrates an Inertial Measurement Unit (IMU) BNO055 (Bosch, Germany) placed on the foot tip. This sensor runs to 60 Hz, using the angular velocity and acceleration to trigger the device. Specifically, for gait assistance, an algorithm based on machine learning estimates the user’s gait phases in real-time [43]. Notwithstanding, for the stationary therapy, a statistical algorithm determines the user’s movement intention.

For the processing, the exoskeleton uses a Raspberry Pi 3 Board under a Debian operating system. This computer acquires sensor information, runs the control algorithms, and sends the control commands to the actuators. Finally, in the power supply context, the device has a LiPo battery of 4000 mah 4S 14.8V 30C, which allows an autonomy close to 4 h in non-extreme conditions (i.e., high level of spasticity and excessive strain on the tendons or stiff filaments).

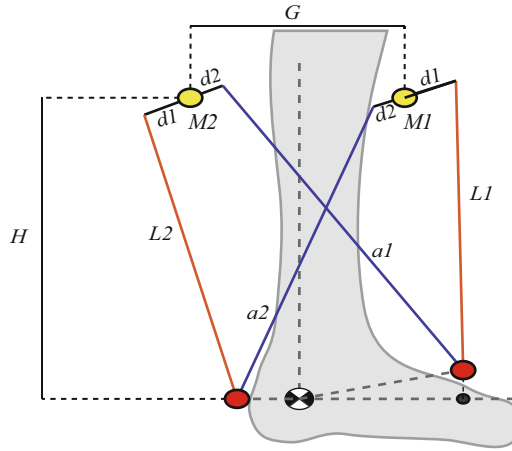


Fig. 7.5 Mechanical diagram of the T-FLEX exoskeleton implemented in the user’s limb conditioned to the anthropometric measurements. The device includes two actuators, i.e., anterior (M1) and posterior (M2), placed on the shank and distanced by the user’s body compositions (G). The exhibited parameters are elastic elements’ length (i.e., L1 for the anterior tendon and L2 for the posterior), stiff element’ lengths (i.e., a1 for the filament attached from M2 to the foot tip, and a2 for the filament from the M1 to the heel), the distance between the actuators and the ankle joint (H), and finally, the attachment systems’ dimensions for the elastic and stiff elements, i.e., d1 and d2, respectively

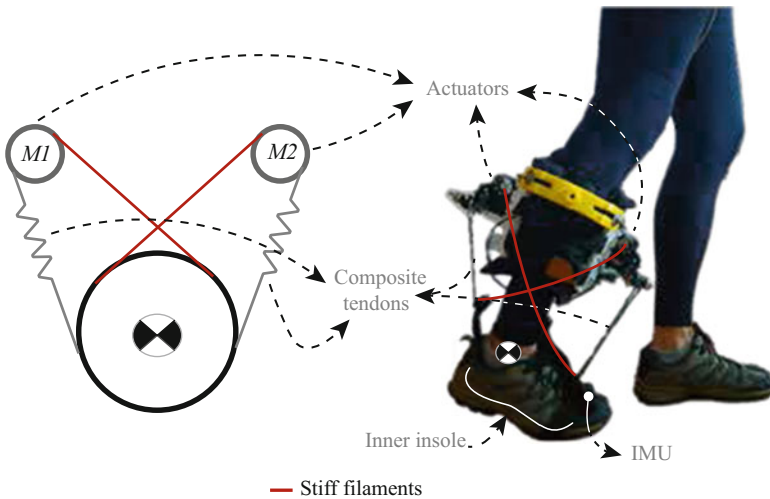


Fig. 7.6 Real prototype of the T-FLEX ankle exoskeleton based on a variable stiffness principle

Finally, T-FLEX has a mechatronic model divided into two main parts: (1) actuators controller and (2) mechanical design’s effect. The first part refers to the internal PID controller implemented on each motor. This controller has as input

a goal motor position converted to profiles of velocity and acceleration. The PID controller calculates the PWM output based on those profiles. Finally, an inverter supplies the PWM value to the actuator and an encoder closes the control loop.

The second part covers effects due to the elastic elements' inclusion. Considering the VSA's characteristics, the system response has a dependency on the spring behavior in terms of provided torque and the system's bandwidth. Thus, the composite tendon included in T-FLEX leads to limited bandwidth and actuators' torque reduction. Likewise, these effects depend on each tendon's pretension, during the initial configuration. On the other hand, from the T-FLEX's mechanical design shown in Fig. 7.5, the provided torque on the ankle increases proportionally concerning the user's foot length. Moreover, regarding the assisted movements, the torque in dorsiflexion is more significant than in the plantarflexion movement. This characteristic is because the distance between the ankle and the foot part, where the torque is transmitted is different (see Fig. 7.5). The torque for each movement can be simplified as shown in Eqs. 7.2 and 7.3.

$$\tau_{dorsiflexion} = (F_{M1} - F_{tendon}) \cdot \cos \alpha_1 \cdot L_m + F_{M2} \cdot \cos \alpha_2 \cdot L_m \quad (7.2)$$

$$\tau_{plantarflexion} = (F_{M2} - F_{tendon}) \cdot \cos \alpha_1 \cdot L_h + F_{M1} \cdot \cos \alpha_2 \cdot L_h, \quad (7.3)$$

where L_m and L_h are the distances between the attached tendon position and the ankle joint, α_1 and α_2 are the angles between the attached tendon position and the motor lever arm, F_{tendon} is the loss force related to the elastic element, and F_{M1} and F_{M2} are the provided forces by the motors expressed as

$$F_{1,2} = \frac{\tau_{motor(1,2)}}{d_{1,2}}. \quad (7.4)$$

Considering the mechanical and electronic design of T-FLEX presented previously, the following sections show two preliminary validations of the device in real scenarios. This way, from the wearable robotics' multi-functionality, these validations include experiments in both applications: (1) stationary therapy and (2) gait assistance with healthy people.

7.4 Experimental Validations of the T-FLEX

Wearable devices based on VSA exhibit advantages for rehabilitation and assistive scenarios, as previous sections stated. Specifically, those devices show benefits in aspects such as (1) multimodality, (2) variable physical interaction adjustable to the user performance, and (3) actuation systems based on the human body. Considering these advantages, VSAs are widely recommended for robotic applications where the device interacts intensively with humans [19, 24]. Specifically, studies have

evidenced metabolic cost' reductions related to the changing stiffness level of the actuator [24].

On the other hand, preliminary studies have shown the significant potential of the T-FLEX ankle exoskeleton in rehabilitation scenarios for (1) stationary therapy and (2) gait assistance. For the therapy, a stroke survivor evidenced improvements in the ankle kinematics and spatiotemporal parameters after a rehabilitation process during 18 sessions [44]. Likewise, in terms of gait assistance, the study exhibited relevant outcomes related to the lower-limb kinematics when stroke patients wore the T-FLEX's actuation system [45].

In this context, this section presents two validations of the T-FLEX ankle exoskeleton in rehabilitation scenarios (i.e., stationary therapy and gait assistance). This device is a wearable and portable powered ankle-foot orthosis that applies bioinspiration concepts based on a variable stiffness actuators principle under an agonist-antagonist configuration (see Fig. 7.6), as extensively presented in the previous section.

7.4.1 T-FLEX in Gait Assistance

Considering the T-FLEX's applications, this section presents the experimental validation of this ankle exoskeleton for assistive applications in gait. Thus, the proposed protocol aimed at assessing the first-use condition with T-FLEX to analyze the effect on the user's kinematics during walking over a treadmill.

The experimental validation consisted of assessing the T-FLEX's first-use effect in a healthy subject. This way, the protocol included three modes: (1) no device, (2) unpowered, and (3) powered. For the three modalities, an Electromyography (EMG) sensor (Shimmer, Ireland) measured the muscular activity on the participant's gastrocnemius and tibialis anterior muscles (see Fig. 7.7). Likewise, a G-Walk sensor (BTS Bioengineering, Italy), placed on L5, estimated the spatiotemporal parameters during the trials. Finally, an inertial sensor (Shimmer, Ireland) measured the ankle's kinematics in the actuated limb side. This sensor was located on the participant's foot tip, as Fig. 7.7 shows.

The participant performed three trials of 6 minutes over a treadmill: (1) no device, (2) unpowered, and (3) powered. Moreover, a previous stage, where the volunteer accomplished three 10-meter walk tests to estimate the average walking speed, was included. Thus, the treadmill was configured to this speed value for the different executed modalities. In the first trial, the participant walked over the treadmill without wearing the device. The data acquired in this modality was used as the reference for the other modalities. For the second trial, the user wore the T-FLEX exoskeleton, although the actuators were deactivated. Finally, in the third trial, the participant walked with the device powered and assisting the user gait phases.

This experiment also included an additional calibration stage to adjust the device's mechanical structure to the user's anthropometric measurements for the assisted gait mode. Likewise, this stage allowed configuring the T-FLEX's movements concerning the user's range of motion (ROM).

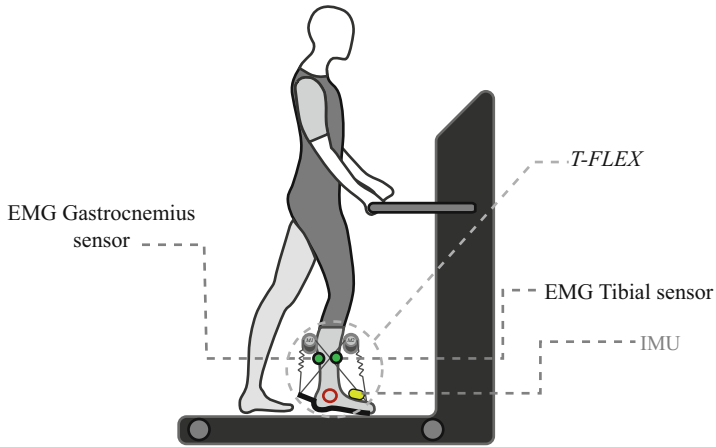


Fig. 7.7 Experimental setup for the validation in a gait assistance application on the treadmill

Data processing was performed offline using the MATLAB software (MathWorks, 2018b, USA) and information acquired through the rosbag package within the ROS operating system framework. Thus, for the acquisition and processing, the HP Pavilion Gaming laptop (IntelCore i5-8300H, CPU@2.30 GHz, Taiwan) was used, running Windows 10 Home. On the one hand, in terms of kinetic parameters, the G-Studio software (BTS Bioengineering, USA) estimated the user performance during trials. On the other hand, for the EMG information, a band-pass filter was applied to remove noise.

The most relevant kinematic parameters are summarized in Fig. 7.8. The device's inclusion in the passive mode shows a decrease in the ankle's ROM. Specifically, the dorsiflexion and plantarflexion exhibited reductions greater than 10% concerning the no-device condition.

This behavior responds to the spring's pretension in the variable stiffness system implemented in T-FLEX. This way, although the mechanical structure does not restrict the user's movements completely, the interaction force between the tendons and the foot is enough to reduce the dorsi-plantarflexion during gait. Consequently, the cadence and the gait cycle exhibited slight changes, and the step length showed increases to compensate for the mentioned reductions. In contrast, when the T-FLEX exoskeleton assisted the user's gait, the dorsi-plantarflexion movements increased concerning the baseline state. Specifically, these movements exhibited increases from 10% to 16%, which could be related to suitable foot-ground contact on the heel strike phase. Likewise, the dorsiflexion's variation for this mode indicates improvements in foot clearance during the swing phase, resulting in a fall risk reduction [44].

On the other hand, this modality also showed reductions in cadence and step length, increasing the user's gait cycle duration. These variations could be associated with the training's lack in the experimental procedure. Thus, multiple sessions with

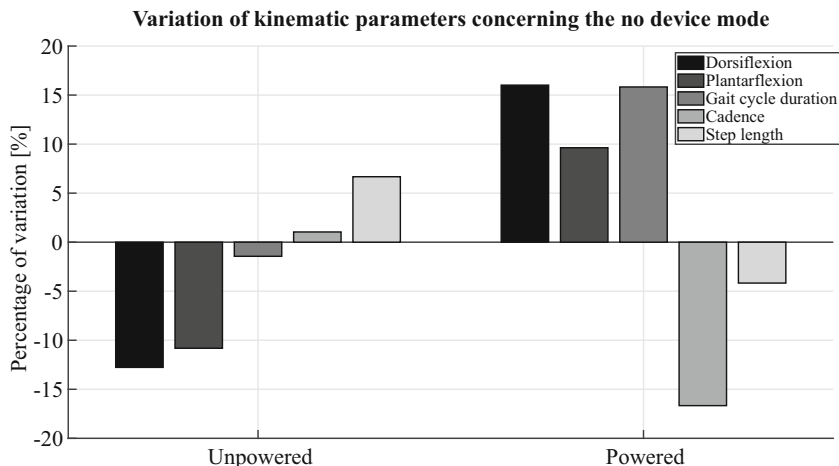


Fig. 7.8 Percentage variation of the kinematic parameters registered during the assistance with T-FLEX. The values were estimated concerning the baseline (i.e., no-device condition). Positive values indicate increases in the parameter, and negative values evidence decreases

the exoskeleton could improve the user–device adaptability until achieving at least values determined in the baseline state.

In the muscular activity context, Fig. 7.9 shows the variations in the gastrocnemius and tibialis anterior muscles. In general terms, the unpowered condition exhibited no significant changes (i.e., less than 10%) in the measured electrical activity concerning the no-device condition. Thus, it could be inferred that the T-FLEX exoskeleton does not cause an additional effort in the patient related to the device’s weight and the mechanical structure.

On the other hand, the powered mode (i.e., T-FLEX assisting user gait) showed (1) an increase in the tibialis anterior and (2) a reduction in the gastrocnemius muscle (see Fig. 7.9). This way, these variations relate to the variable stiffness system’s effects and the device’s assistance capacity. Specifically, the change in the dorsiflexion movement could increase the tibialis anterior’s electrical activity. Moreover, the EMG’s reduction in the gastrocnemius could indicate that T-FLEX assisted the leg propulsion during the toe-off phase.

7.4.2 T-FLEX in a Stationary Scenario

This section shows a preliminary validation of the device under a stationary condition from the T-FLEX’s applicability in rehabilitation scenarios. This way, the proposed experimental protocol was intended to measure the muscular activity response in a healthy subject using the exoskeleton.

The experimental protocol’s goal intended to assess the device’s effect during a stationary therapy scenario, measuring the user’s EMG and ROM (see Fig. 7.10). To

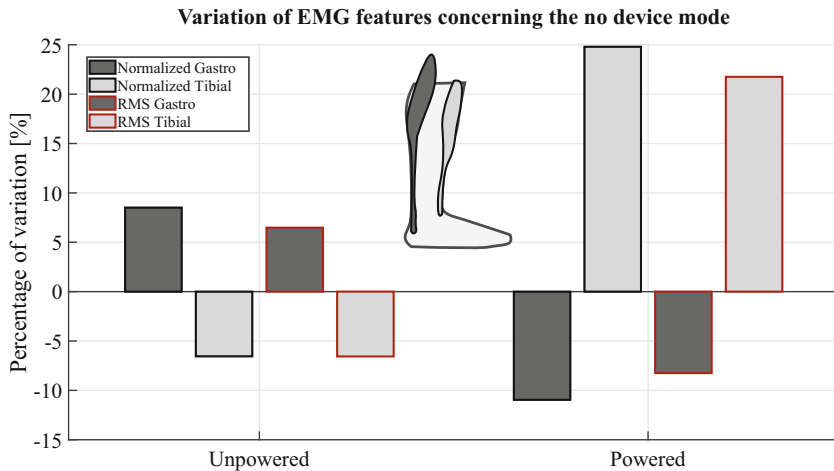


Fig. 7.9 Percentage variation of the electrical activity measured on the gastrocnemius and tibialis anterior muscle during the gait assistance. The values were estimated concerning the no-device condition. Positive values indicate an increase in the EMG, and negative values a decrease

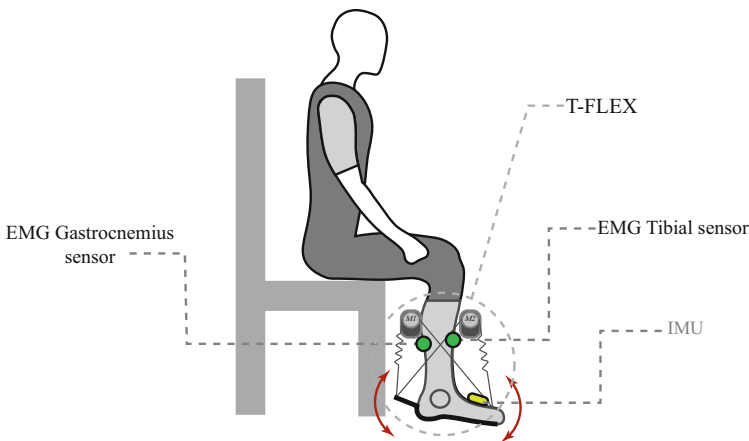


Fig. 7.10 Experimental setup proposed to assess the T-FLEX exoskeleton in a stationary application

this end, this study enrolled a healthy participant who had no exhibited orthopedic, metabolic, or neurological impairment that could modify his muscular activity. The participant was equipped with electrodes located on the tibialis anterior and gastrocnemius muscles on their dominant side. Likewise, two inertial sensors (Shimmer, Ireland) were placed on their foot instep and at the shank (i.e., 10 cm on the tibia proximal to the ankle joint). Subsequently, the user wore the T-FLEX exoskeleton as Fig. 7.10 shows.

For this study, T-FLEX was configured in therapy mode, where the device assists the dorsi-plantarflexion movements concerning the user's ROM, the actuators' velocity, and the repetition frequency. Moreover, the participant was asked to sit in a 90-degree knee flexion with his dominant lower limb elevated without contact with the ground.

This study included one session divided into two modalities: (1) no-device condition and (2) T-FLEX assisting the dorsi-plantarflexion movements. For the first modality, the user accomplished continuous dorsi-plantarflexion repetitions with a self-determined speed and a repetition frequency of 0.8 Hz. This trial was used as a baseline for the other assessed modality. The second modality integrated three tests where the device assisted the ankle movements with different speeds. Thus, the continuous repetitions had an actuator's velocity of 30% (low), 50% (medium), and 100% (high) concerning the maximum device's speed (i.e., 55 rpm for the no-load condition). Likewise, the set-point commands were sent to the actuators to achieve a repetition frequency of 0.8 Hz.

Data processing was performed offline using MATLAB software (MathWorks, 2018b, USA) and an Asus VivoBook S15 S510UA (IntelCore i5-8250U, CPU@1.80 GHz, Taiwan) running Windows 10 Home. For the processing, a band-pass filter removed the atypical values and noise in the EMG signals. Subsequently, the signals were rectified (i.e., from the absolute values), and data smoothing was performed using a 100 ms motion average window. Finally, to provide information about the EMG signal's amplitude during the trials, the root-mean-square (RMS) was calculated.

The muscular activity measured on the tibialis anterior evidenced a significant decrease for all assisted trials (i.e., low, medium, and high), as Fig. 7.11 shows. Specifically, the exhibited reduction was 93% for the low velocity, being the maximum value obtained in the experiment. However, the muscular activity measured on the gastrocnemius muscle presented its maximum variation in this trial (i.e., 270% concerning the baseline state).

On the other hand, medium and high velocities led to a shorter increase in the gastrocnemius' electrical activity, although the tibialis anterior evidenced a slight increase compared to the low speed. This way, the device's speed evidenced a relevant impact on the user's electrical activity. In general, when T-FLEX assisted the movements with a low velocity, the participant registered significant increases in gastrocnemius' activity. However, as the actuators' speed is increased, the electrical activity reached similar values obtained in the baseline state. In contrast, the tibialis anterior showed a significant decrease for all trials, which could be related to the user's posture and the T-FLEX's assistance capacity.

In the user's ROM context, Fig. 7.12 shows the values obtained in the sagittal plane for the baseline (passive) and assisted motion (active) modalities. The user's ROM exhibited a decrease of 11.9% when T-FLEX supported the dorsi-plantarflexion in the different velocities.

This result can be explained by the elongation of the spring while the device assists the movement (see Fig. 7.12), resulting in a position set-point loss. Therefore, a high level of pretension could improve the reduced ROM registered by the device.

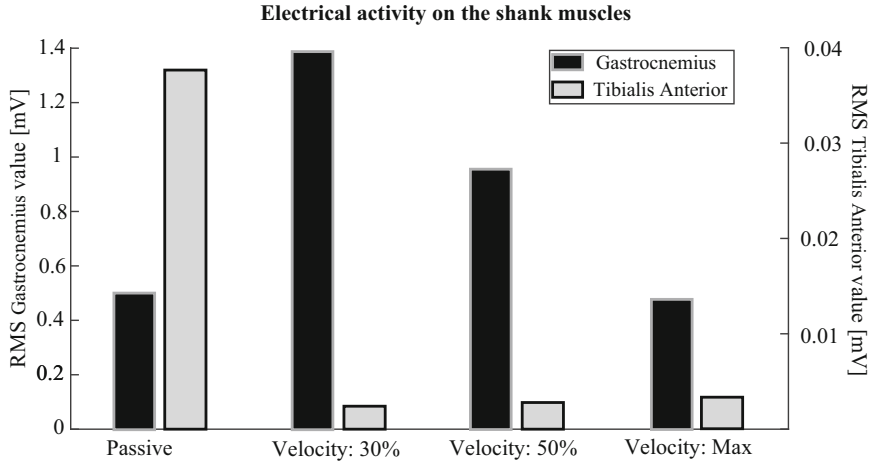


Fig. 7.11 RMS values of the EMG signals acquired for tibialis anterior and gastrocnemius muscles in the proposed trials. The velocity's percentage was configured concerning the actuators' maximum speed (i.e., 55 rpm in a no-load state)

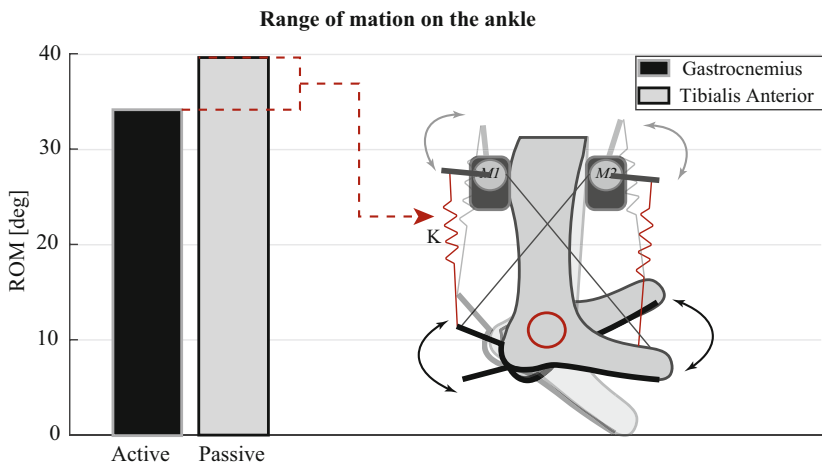


Fig. 7.12 Range of Motion on the ankle joint for the sagittal plane during the assessed modalities, i.e., active and passive. The left part shows the values for the dorsi-plantarflexion movements, and the right part shows the effect on these movements related to the element's elasticity (K)

Additionally, this reduction can also be related to the calibration methodology used for this experiment, i.e., storing the user's ROM and employing these values in the exercise. Hence, an automated calibration, including a sensor to measure the user's current state, could improve these values.

7.5 Conclusions

This chapter presented an overview of the variable stiffness actuators (VSAs) in terms of principles, setups, and characteristics applied to assistive applications. In this sense, it also presented an ankle exoskeleton T-FLEX based on VSA, focusing on its mechanical design and operating principles during gait assistance and stationary therapy. Likewise, this chapter showed two preliminary studies of healthy participants using T-FLEX in these scenarios.

In conclusion, devices based on VSA evidence advantages in assistive applications compared to other actuation mechanisms. Moreover, in a rehabilitation context, the application of these systems, integrating bioinspired concepts and modifying its performance concerning the user's capabilities, enables to improve the physical interaction. However, aspects as the design, control, and integration of these devices in real scenarios could be challenged and require further research.

References

1. M. Zhang, T.C. Davies, S. Xie, Effectiveness of robot-assisted therapy on ankle rehabilitation—a systematic review. *J. NeuroEng. Rehab.* **10**(1), 30 (2013)
2. G. Onose, V. Cârdei, Ş.T. Crăciunoiu, V. Avramescu, I. Opreş, M.A. Lebedev, M.V. Constantinescu, Mechatronic wearable exoskeletons for bionic bipedal standing and walking: a new synthetic approach. *Front. Neurosci.* **10**, 343 (2016)
3. J.-M. Belda-Lois, S. Mena-del Horno, I. Bermejo-Bosch, J.C. Moreno, J.L. Pons, D. Farina, M. Iosa, M. Molinari, F. Tamburella, A. Ramos. et al., Rehabilitation of gait after stroke: a review towards a top-down approach. *J. NeuroEng. Rehab.* **8**(1), 66 (2011)
4. M. Moltedo, T. Baček, T. Verstraten, C. Rodriguez-Guerrero, B. Vanderborght, D. Lefeber, Powered ankle-foot orthoses: the effects of the assistance on healthy and impaired users while walking. *J. NeuroEng. Rehab.* **15**, 86 (2018)
5. B. Chen, H. Ma, L.-Y. Qin, F. Gao, K.-M. Chan, S.-W. Law, L. Qin, W.-H. Liao, Recent developments and challenges of lower extremity exoskeletons. *J. Orthopaedic Transl.* **5**, 26–37 (2016)
6. H.P. Crowell III, A.C. Boynton, M. Mungiole, Exoskeleton power and torque requirements based on human biomechanics, tech. rep., Army Research Lab Aberdeen Proving Ground Md, 2002
7. A. Weerasingha, W. Withanage, A. Pragnathilaka, R. Ranaweera, R. Gopura, Powered Ankle exoskeletons: Existent designs and control systems. *Proc. Int. Conf. Artif. Life Robot.* **23**, 76–83 (2018)
8. M. Alam, I.A. Choudhury, A.B. Mamat, Mechanism and design analysis of articulated ankle foot orthoses for drop-foot. *Sci. World J.* **2014**, 1–14 (2014)
9. S. Sierra, L. Arciniegas, F. Ballen-Moreno, D. Gomez-Vargas, M. Munera, C.A. Cifuentes, Adaptable robotic platform for gait rehabilitation and assistance: Design concepts and applications. *Exoskeleton Robot. Rehab. Healthcare Dev.* 67–93 (2020)
10. A. Petcu, M. Georgescu, D. Tarniţă, Actuation systems of active orthoses used for gait rehabilitation. *Appl. Mech. Mater.* **880**, 118–123 (2018)
11. K. Kong, J. Bae, M. Tomizuka, A compact rotary series elastic actuator for human assistive systems. *IEEE/ASME Trans. Mechatron.* **17**(2), 288–297 (2011)
12. S. Toxiri, A. Calanca, T. Poliero, D.G. Caldwell, J. Ortiz, Actuation requirements for assistive exoskeletons: Exploiting knowledge of task dynamics, in *International Symposium on Wearable Robotics* (Springer, 2018), pp. 381–385

13. G.A. Pratt, M.M. Williamson, Series elastic actuators, in *Proceedings 1995 IEEE/RSJ International Conference on Intelligent Robots and Systems. Human Robot Interaction and Cooperative Robots*, vol. 1 (IEEE, 1995), pp. 399–406
14. S. Wolf, G. Grioli, O. Eiberger, W. Friedl, M. Grebenstein, H. Höppner, E. Burdet, D.G. Caldwell, R. Carloni, M.G. Catalano, et al., Variable stiffness actuators: Review on design and components. *IEEE/ASME Trans. Mechatron.* **21**(5), 2418–2430 (2015)
15. N. Hogan, Impedance control: An approach to manipulation, in *1984 American Control Conference* (IEEE, 1984), pp. 304–313
16. R. Van Ham, T.G. Sugar, B. Vanderborght, K.W. Hollander, D. Lefeber, Compliant actuator designs. *IEEE Robot. Autom. Mag.* **16**(3), 81–94 (2009)
17. B. Vanderborght, A. Albu-Schäffer, A. Bicchi, E. Burdet, D. G. Caldwell, R. Carloni, M. Catalano, O. Eiberger, W. Friedl, G. Ganesh. et al., Variable impedance actuators: A review. *Robot. Autonom. Syst.* **61**(12), 1601–1614 (2013)
18. F. Petit, M. Chalon, W. Friedl, M. Grebenstein, A. Albu-Schäffer, G. Hirzinger, Bidirectional antagonistic variable stiffness actuation: Analysis, design & implementation, in *2010 IEEE International Conference on Robotics and Automation* (IEEE, 2010), pp. 4189–4196
19. P.K. Jamwal, S. Hussain, S.Q. Xie, Review on design and control aspects of ankle rehabilitation robots. *Disability Rehab. Assist. Tech.* **10**, 93–101 (2013)
20. L. Marchal-Crespo, D.J. Reinkensmeyer, Review of control strategies for robotic movement training after neurologic injury. *J. NeuroEng. Rehab.* **6**, 20 (2009)
21. E. Rocon, J.L. Pons, *Exoskeletons in Rehabilitation Robotics: Tremor Suppression*, vol. 69 (Springer, 2011)
22. M.D.C. Sanchez-Villamañan, J. Gonzalez-Vargas, D. Torricelli, J.C. Moreno, J.L. Pons, Compliant lower limb exoskeletons: A comprehensive review on mechanical design principles. *J. NeuroEng. Rehab.* **16**(1), 1–16 (2019)
23. M. Moltedo, G. Cavallo, T. Baček, J. Lataire, B. Vanderborght, D. Lefeber, C. Rodriguez-Guerrero, Variable stiffness ankle actuator for use in robotic-assisted walking: Control strategy and experimental characterization. *Mech. Mach. Theory* **134**, 604–624 (2019)
24. M. Moltedo, T. Baček, B. Serrien, K. Langlois, B. Vanderborght, D. Lefeber, C. Rodriguez-Guerrero, Walking with a powered ankle-foot orthosis: the effects of actuation timing and stiffness level on healthy users. *J. NeuroEng. Rehab.* **17**(1), 1–15 (2020)
25. G. Carpino, D. Accoto, F. Sergi, N. Luigi Tagliamonte, E. Guglielmelli, A novel compact torsional spring for series elastic actuators for assistive wearable robots. *J. Mech. Des.* **134**, 1–10 (2012)
26. M.A. Dimyan, L.G. Cohen, Neuroplasticity in the context of motor rehabilitation after stroke. *Nature Rev. Neurol.* **7**(2), 76–85 (2011)
27. L.R. Sheffler, J. Chae, Technological advances in interventions to enhance poststroke gait. *Phys. Med. Rehab. Clin. North America* **24**, 305–323 (2013)
28. T. Mikolajczyk, I. Ciobanu, D.I. Badea, A. Iliescu, S. Pizzamiglio, T. Schauer, T. Seel, P.L. Seiciu, D.L. Turner, M. Berceanu, Advanced technology for gait rehabilitation: An overview. *Adv. Mech. Eng.* **10**(7), 1–19 (2018)
29. R. Van Ham, B. Vanderborght, M. Van Damme, B. Verrelst, D. Lefeber, MACCEPA, the mechanically adjustable compliance and controllable equilibrium position actuator: Design and implementation in a biped robot. *Robot. Autonom. Syst.* **55**(10), 761–768 (2007)
30. M. Cestari, D. Sanz-Merodio, J.C. Arevalo, E. Garcia, An adjustable compliant joint for lower-limb exoskeletons. *IEEE/ASME Trans. Mechatron.* **20**(2), 889–898 (2014)
31. T. Bacek, M. Moltedo, K. Langlois, G.A. Prieto, M.C. Sanchez-Villamañan, J. Gonzalez-Vargas, B. Vanderborght, D. Lefeber, J.C. Moreno, Biomot exoskeleton—towards a smart wearable robot for symbiotic human-robot interaction, in *2017 International Conference on Rehabilitation Robotics (ICORR)* (IEEE, 2017), pp. 1666–1671
32. P. Cherule, V. Grosu, P. Beyl, A. Mathys, R. Van Ham, M. Van Damme, B. Vanderborght, D. Lefeber, The MACCEPA actuation system as torque actuator in the gait rehabilitation robot ALTACRO, in *2010 3rd IEEE RAS & EMBS International Conference on Biomedical Robotics and Biomechatronics* (IEEE, 2010), pp. 27–32

33. B. Brackx, J. Geeroms, J. Vantilt, V. Grosu, K. Junius, H. Cuypers, B. Vanderborght, D. Lefeber, Design of a modular add-on compliant actuator to convert an orthosis into an assistive exoskeleton, in *5th IEEE RAS/EMBS International Conference on Biomedical Robotics and Biomechatronics* (IEEE, 2014), pp. 485–490
34. K. Junius, B. Brackx, V. Grosu, H. Cuypers, J. Geeroms, M. Moltedo, B. Vanderborght, D. Lefeber, Mechatronic design of a sit-to-stance exoskeleton, in *5th IEEE RAS/EMBS International Conference on Biomedical Robotics and Biomechatronics* (IEEE, 2014), pp. 945–950
35. M. Cestari, D. Sanz-Merodio, J.C. Arevalo, E. Garcia, Ares, a variable stiffness actuator with embedded force sensor for the atlas exoskeleton. *Ind. Robot Int. J.* **41**(6), 518–526 (2014)
36. J. Sancho-Perez, M. Perez, E. Garcia, D. Sanz-Merodio, A. Plaza, M. Cestari, Mechanical description of atlas 2020, a 10-dof paediatric exoskeleton, in *Advances in Cooperative Robotics* (World Scientific, 2017), pp. 814–822
37. N.G. Tsagarakis, I. Sardellitti, D.G. Caldwell, A new variable stiffness actuator (compAct-VSA): Design and modelling, in *2011 IEEE/RSJ International Conference on Intelligent Robots and Systems* (IEEE, 2011), pp. 378–383
38. A. Jafari, N.G. Tsagarakis, D.G. Caldwell, AwAS-II: A new actuator with adjustable stiffness based on the novel principle of adaptable pivot point and variable lever ratio, in *2011 IEEE International Conference on Robotics and Automation* (IEEE, 2011), pp. 4638–4643
39. A. Jafari, N.G. Tsagarakis, I. Sardellitti, D.G. Caldwell, A new actuator with adjustable stiffness based on a variable ratio lever mechanism. *IEEE/ASME Trans. Mechatron.* **19**(1), 55–63 (2012)
40. M. Sánchez-Manchola, D. Gómez-Vargas, D. Casas-Bocanegra, M. Múnera, C. A. Cifuentes, Development of a robotic lower-limb exoskeleton for gait rehabilitation: Agora exoskeleton, in *2018 IEEE ANDESCON* (IEEE, 2018), pp. 1–6
41. M. Manchola, D. Serrano, D. Gómez, F. Ballen, D. Casas, M. Munera, C.A. Cifuentes, T-flex: Variable stiffness ankle-foot orthosis for gait assistance, in *International Symposium on Wearable Robotics* (Springer, 2018), pp. 160–164
42. J. Casas, A. Leal Junior, C. Díaz, A. Frizera, M. Munera, C. Cifuentes, Large-range polymer optical-fiber strain-gauge sensor for elastic tendons in wearable assistive robots. *Materials* **12**, 1443 (2019)
43. M.D. Sánchez Manchola, M.J.P. Bernal, M. Munera, C.A. Cifuentes, Gait phase detection for lower-limb exoskeletons using foot motion data from a single inertial measurement unit in hemiparetic individuals. *Sensors* **19**(13), 2988 (2019)
44. D. Gomez-Vargas, M.J. Pinto-Betnal, F. Ballén-Moreno, M. Múnera, C.A. Cifuentes, Therapy with t-flex ankle-exoskeleton for motor recovery: A case study with a stroke survivor, in *2020 8th IEEE RAS/EMBS International Conference for Biomedical Robotics and Biomechatronics (BioRob)* (IEEE, 2020), pp. 491–496
45. D. Gomez-Vargas, F. Ballen-Moreno, P. Barria, R. Aguilar, J.M. Azorín, M. Munera, C.A. Cifuentes, The actuation system of the ankle exoskeleton t-flex: First use experimental validation in people with stroke. *Brain Sciences* **11**(4), 412 (2021)